

# A Prognostic Model for Predicting Liver Cancer Patients found On Immune Checkpoint Gene-Related Basement Membrane Genes, And Analyzing Immunity and Potential Drug Candidates

Yiyang Chen<sup>1</sup>, Yiju Gong<sup>2</sup>, Xi Ou<sup>3</sup>

## Abstract

**Objective:** Among the most prevalent malignant tumours globally, liver cancer has a high fatality rate. The incidence rate has risen steadily in recent years. Tumors cannot be removed by the immune system because immunological checkpoint genes are expressed in tumour cells. Basement membrane-related genes are the genes closely related to human diseases obtained by the latest research.

**Methods:** First, immune checkpoint genes were used to extract genes associated to the basement membrane, and a prognostic model of immune checkpoint genes connected to the basement membrane was created. Survival analysis, progression-free survival analysis, and independent prognostic analysis were used to generate the C-index curves and ROC. The clinical grouping model's accuracy was verified using curves, principal component analysis, and validation. To further investigate the model's potential use, enrichment analysis, immunological analysis, and tumour mutation burden survival analysis were carried out. Finally, discussion of prospective medication targeting models follows.

**Results:** A prognostic model was developed, and its accuracy in predicting patients' survival times from liver cancer was confirmed. The distinct functions and pathways of differential genes were discovered by GO and KEGG enrichment analysis. Four immune functions differentially expressed were found. The most altered genes in the both risk groups were analyzed. The research examined at 25 different drugs, with considerable differences in drug sensitivity across high- and low-risk groups.

**Conclusion:** It offers new insights and methodologies for the survival prediction of liver cancer patients as well as the development of immune-tailored therapies by examining the relationship between immune checkpoint gene-associated basement membrane genes and the prognosis and immunity of liver cancer patients.

**Keywords:** immune checkpoint gene, basement membrane, liver cancer, immunity

**Citation:** Chen Y, Gong Y, Qu X. A Prognostic Model for Predicting Liver Cancer Patients found On Immune Checkpoint Gene-Related Basement Membrane Genes, And Analyzing Immunity and Potential Drug Candidates [Online]. *Annals ASH KMDC* 2022;27:

(ASH & KMDC 27(4):191;2022)

## Introduction

Among the most common malignant tumours around the world, liver cancer has a high mortality rate<sup>1</sup>. The prognosis is poor since it is difficult to identify early and easy to transfer. The usual treatment for liver cancer is surgical resection. According to research, liver cancer is an inflammation-related tumor with a distinct immunosuppressive mi

croenvironment<sup>2-3</sup>. Immune checkpoint gene expression often reduces autoimmune reactivity, and its presence in tumor cells stops the immune system from clearing malignancies<sup>4</sup>. Furthermore, immunological checkpoint genes (ICGs) represent novel targets for cancer therapeutic development<sup>5</sup>. The basement membrane (BM) is the oldest extracellular matrix (ECM) in animals and is made up of several components. According to research, the variation of more than 20 basement membrane genes highlights their diversity and basic activities, which are at the root of human disorders<sup>6</sup>. Basement membrane proteins are autoantibody targets in immunological disorders, and abnormalities in basem-

<sup>1-3</sup> Peking University Shenzhen hospital

### Correspondence:

Xi O Peking University Shenzhen hospital, China

Email: [bdszyox@163.com](mailto:bdszyox@163.com)

Date of Submission: 28<sup>th</sup> October 2022

Date of Acceptance: 29<sup>th</sup> November 2022

ent membrane protein production and turnover can contribute to cancer<sup>7,8</sup>. In this study, genes associated to basement membrane genes were identified from immune checkpoint-related genes, and a liver cancer prognostic model was built using basement membrane genes connected to immune checkpoint genes.

## Patients and Methods

### Data Sources

The sample size for this study was established using all liver cancer patient samples available in the TCGA database. Genes related to immunological checkpoints and genes for the basement membrane were gathered from previously published studies. The TCGA database, associated clinical feature data, mutation data of the RNA sequence of liver cancer patients were used in this work to obtain transcriptome data. Clinical information was retrieved from the transcriptome data after mRNA and lnc-RNA were separated. Tumor Mutational Burden Calculation Furthermore, the most recent research discovered 224 basement membrane-related genes<sup>9</sup> and 79 immune checkpoint-related genes<sup>5</sup> that are strongly linked to human disorders. To extract their linked expression matrix, immune checkpoint genes and basement membrane-related genes were coupled with mRNA from liver cancer. The basement membrane genes that are linked with immune checkpoint genes were discovered using the limma package in R studio program. We selected a correlation coefficient benchmark of 0.3 for this experiment. It was believed that a correlation coefficient greater than 0.3 was statistically significant. Immune checkpoints, 0.3, and  $p < 0.05$  for genes were thought to be favorably linked with basement membrane genes. Finally, an expression matrix of basement membrane genes related with immunological checkpoints was obtained and used for further investigation.

### Model building

First, the liver cancer expression matrix of basement membrane genes related to immune checkpoint genes was integrated with clinical data from liver cancer patients (survival status and survival

time). The prognostic model was created using the R studio software packages “survival,” “caret,” “glmnet,” and “survminer” after merging the expression. A model was created with 0.5 for each of the train and test groups after the data had been grouped once, and a univariate cox analysis was carried out on the train group data to find prognostic genes. Then, using the single-factor significant basement membrane genes related to immune checkpoints, perform lasso regression analysis, cross-validate to find the point with the smallest lasso regression error, and build a COX model for the genes gained by lasso regression and output the model formula. The train group was separated into two categories, based on the median value of the risk score low risk and high risk, which was calculated using the model formula. In order to determine whether the clinical traits of the training and test groups were different, a clinical statistical analysis was carried out simultaneously on the two groups.

### Model validation

With the help of “survival” and “survminer” packages in R Studio the survival difference between the two risk groups was examined, and the findings produced a significant P value. A contemporaneous differential analysis of the progression-free survival of all patients was performed in order to compare PFS between the low risk and high risk groups. Risk curves for the train and test groups were produced using the “pheatmap” application. It may be evaluated if the risk score can be used as an independent prognostic factor for patients with liver cancer, independent of other factors, by independent prognostic analysis, both univariate and multivariate. The model’s accuracy in forecasting the 1-, 3-, and 5-year patients’ survival with liver cancer was assessed using ROC curve analysis. The accuracy of the models created in this study was evaluated by comparing the risk scores to other clinical variables using C-index curves. The “survival” and “survminer” programmes are used to validate the clinical grouping model created in this study to see if patients with early-stage and advanced liver cancer should use it. Using the scatterplot3d feature of the R studio software, principal

component analysis was used to determine whether the genes involved in model construction could classify patients into two risk categories i.e., high and low.

### **Immune and gene function connection analysis**

To detect distinct genes in the two risk groups, risk differential analysis was first performed using logFC filter conditions of logFCfilter=1 and fdr filter conditions of fdrFilter=0.05. Then, use R studio to run GO and KEGG enrichment analysis to determine which functionality the differentially expressed genes are engaged in. route enrichment is included To determine if patients in the two risk groups had different immune-related functions, immune-related activities were analyzed. Comparing gene mutations' frequency by creating waterfall charts for both risk groups. The survival of the tumour mutational burden was next examined. If there was a survival difference between the two risk groups, it was found using a survival analysis of the tumour mutational burden and the risk score of HCC patients. After that, a combination study of tumour mutational burden and HCC patient risk score was performed. Final step was to test potential treatments for the illness, and the filter condition was set to pvalue:pFilter=0.001. The names of medications with statistically significant differences of sensitivity of drug between the two groups were looked up. Greater drug sensitivity is indicated by a lower IC 50 value.

### **Nomogram construction and validation**

Nomograms were developed in R studio using the survival, rms packages and regplot, to envisage survival rate of 1-year, 3-year, and 5-year patients with liver cancer. Nomogram-predicted test was also employed at the same time. Using the calibration curve, it was determined that the model was accurate in predicting patient survival.

## **Results**

### **Model building**

A prediction model was created by integrating the clinical data (time and status of survival) of liver cancer patients with the expression matrix of 168 basement membrane genes relevant to immun-

ological checkpoints. For the development of a COX model on the basis of immune checkpoint-related basement membrane genes and a Lasso regression of prognostic genes, the combined data was divided among train group (n=185) and a test group (n=185) randomly. The first log rank value with the lowest segmentation error is shown by the vertical dashed line (Fig. 1A and Fig. 1B). Prognostic proteins were chosen as the study group's independent relationships with survival for the creation of risk models to assess the prognostic risk of patients with liver cancer. four immune checkpoint-related basement membrane genes—ADAMTS5, CTSA, FBLN5, and P3H1—were chosen for additional multivariate analysis. The multivariate Cox regression analysis-based prognostic model had the following equation: Score of Risk = (1.2596869 0844101\*ADAMTS5expression)+(0.33298572 9856301\* CTSA expression)+(-0.31683170952125\* FBLN5expression)+(0.346521502281786\*P3H1expression). According to the median score of the prognostic risk grades, the study was split into two risk group; a low risk (PRG score median) and high-risk (PRG score > median) groups. Low-risk genes (blue) and high-risk genes (red) (green).

### **Model validation**

To see if the clinical traits of the train and test groups were different, a clinical statistical analysis was first performed. The results demonstrated that each P value exceeded 0.05. (Table 1). The survival analysis revealed that overall survival between the two groups was statistically significant (Fig. 2A) and low-risk (Fig. 2B) groups, with high-risk group patients experiencing an inferior survival rate. According to the analysis of progression-free survival (Fig 2C), low risk group patients had poor chances of survival than those in the general population. The death rate of patients with liver cancer grows as the risk score rises, according to hazard curves with risk scores (Panels D and G), survival status (Panels E and H), and risk heatmaps (Panels F and I). The risk heat map score also revealed one low-risk gene, FBLN5, three high-risk genes (ADAMTS5, CTSA, and P3H1).

Independent prognosis analysis to determine whether the model utilised in this study can be used independently of other clinical variables as a prognostic factor. The risk score and 95% confidence interval (CI) exhibited HRs of 1.201 and 1.1321.274, respectively, in the univariate independent prognostic analysis (Figure 3A); and 1.174 and 1.1021.251, respectively, in the multivariate independent prognostic analysis (Figure 3B) (p 0.001). Values for 1 year, 3 years, and 5 years are all more than 0.5, according to the ROC curve in Figure 3C. The model had the largest area under the ROC curve, which was created in Figure 3D by combining it with additional clinical features. In the model developed for this study, the Concordance index has the highest value in Figure 3E's C-index curve. The model developed in this work is suitable for both those with advanced-stage liver cancer and those with early-stage liver cancer, as shown in Figures 3F and 3G. Principal component analysis was used to examine whether the patients could be divided into the two risk categories on the basis of genes used in the model construction. Figure 3H demonstrates that while all genes and immune checkpoint-related genes are unable to distinguish patients in both risk groups, immune checkpoint-related basement membrane genes can identify high and low risk patients (Figure 3I and Figure 3J).

**Gene function and immune correlation analysis**

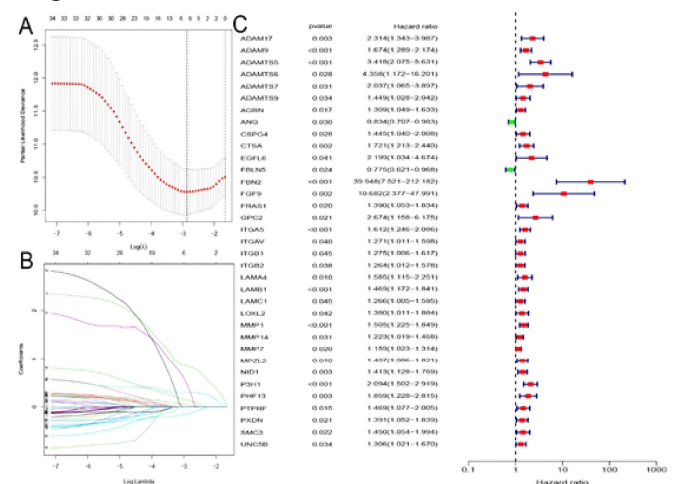
The investigation's next step was to screen the different genes in the two key risks, and 49 differential genes in total were found. The differential genes are predominantly enriched in active transmembrane transporter activity, the basal region of the cell, and the regulation of cyclin-dependent protein kinase activity, according to the GO functional enrichment analysis of the differential genes (Fig 4A). The differential genes were predominantly enriched in cell-substrate adhesion and response to xenobiotic stimuli, according to KEGG pathway enrichment analysis in Figure 4B. An assessment of immune-related processes (Fig 4C). The four immune-related activities that differ significantly be-

tween the two risk groups are Type II IFN Response, Cytolytic activity, MHC class I, and Type I IFN Response, with MHC class I being more active in the high-risk group. (4D and 4E in Figures) The four genes TP53, CTNNB1, TTN, and MUC16 have the highest mutation frequency, with the exception of CTNNB1. This is demonstrated by the waterfall graphs. In comparison among the two groups the high-risk group's mutation frequencies were higher for the other genes. The findings of a survival analysis of tumour mutational burden are shown in Figure 4F. It was demonstrated that patients with a high tumour mutational burden had a considerably poorer rate of survival than those with a low tumour mutational burden. Figure 4G's survival analysis, which combines tumour mutational burden and risk score, shows that patients with the lowest survival rates also have the highest tumour mutational burden and risk scores.

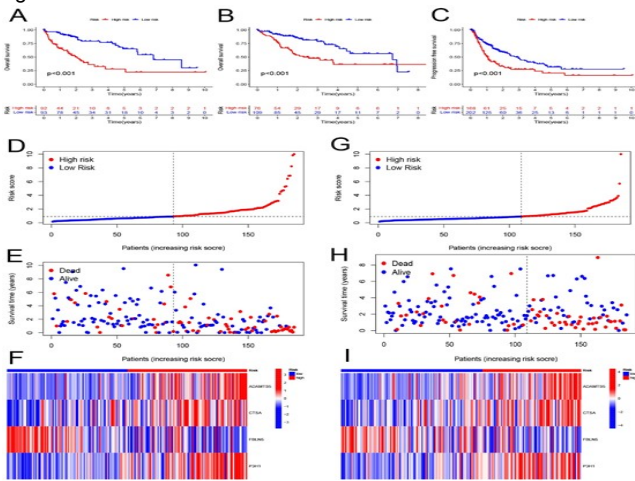
**Nomogram construction, validation and drug sensitivity analysis**

Figure 5A shows a nomogram that was constructed to forecast survival in patients with HCC 1, 3, and 5. The nomogram included risk ratings and clinical indications. The calibration curve in this study demonstrates the great accuracy of the model created to predict the patients' survival at 1, 3, and 5 years (Figure 5B). The sensitivity to 5-Fluorouracil, AKT inhibitor VIII, and bexarotene varied considerably between the two risk groups, as shown in Figure 5C.

**Figure 1**



**Fig 1.** (A) Logarithmic adjustment factors for proteins relevant to survival used in cross-validation of error curves. (B) A LASSO coefficient distribution of the ferroptosis genes linked to OS is shown, along with vertical imaginary lines drawn at values chosen by 10-fold cross-validation; (C) Bas-ement membrane genes linked to immune checkpoints at risk are shown with high and low risk, respectively, with high risk shown in red and low risk in green.



**Fig 2.** (A, B) Patient Kaplan-Meier survival curves for overall survival in the Train and Test groups; (C) comparison of progression-free survival in the high- and low-risk groups. (D,G)The distribution of risk scores between high- and low-risk groups in training and test groups based on progn-ostic models of basement membrane genes associated with immunological checkpoints; (E, H) Survival in training and test groups between high- and low-risk groups. Time and survi-val status; (F, I) heatmaps from a cluster analysis showing the proportions of four immune checkpoint-related basement membrane genes for each patient in the training and testing groups.

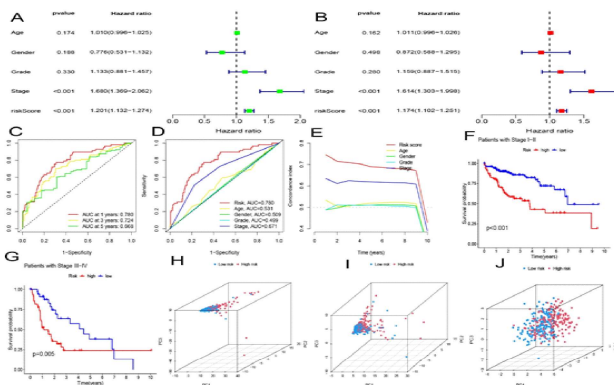


**Fig 3.** (A) A single-variate study of survival risk scores and clinical characteristics. (B) Multivariate analysis of survival risk scores and clinical factors. ROC curves based on clinical characteristics and risk ratings (C, D); C-index curves based on clinical characteristics and risk scores (G, H); (H) Basement membrane genes associated with immunological checkpoints underwent a main component analysis. (I) Principal component analysis of genes related to immunological checkpoints. Principal component analysis across all genes (J).

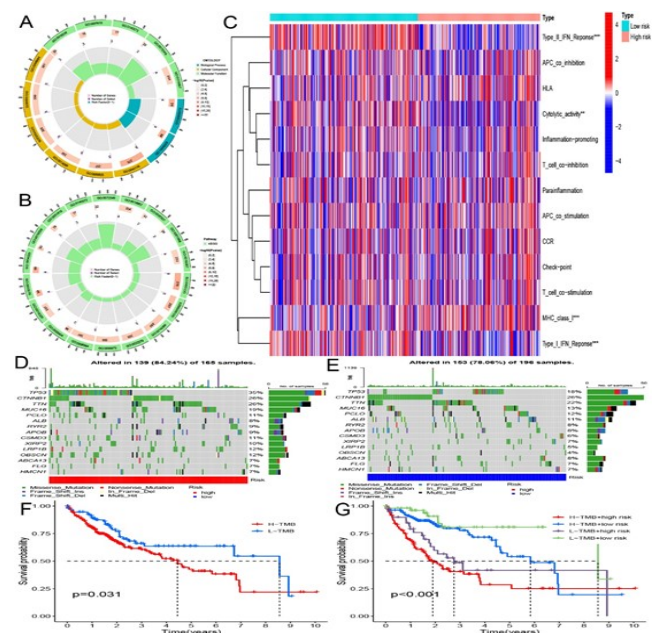


**Fig 4.** (A) Analysis of the differential gene expression between high- and low-risk groups based on GO enrichment. (B) A comparison of the genes in high- and low-risk categories using the KEGG enrichment analysis. (C) Im-mune performance varies between groups at high and low risk. Somatic mutation signa-ture waterfall charts based on high and low risk ratings (D,E) . (F) Kaplan-Meier survival curves for tumor mutation groups with high and low levels; (G) Analysis of tumor mutation load and risk score combined.

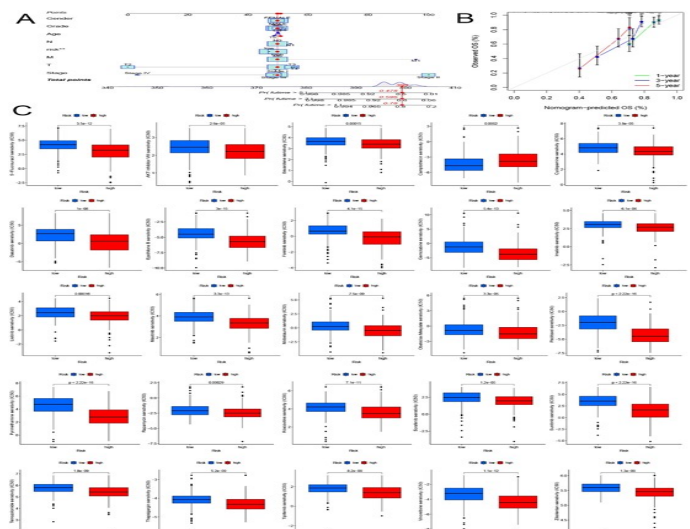


**Fig 5.** Patients with liver cancer types 1, 3, and 5 are shown in (A) a survival nomogram. (B) Test calibration curve anticipated by a nomogram. (C) 25 medications in the high- and low-risk groups with significant drug sensitivity variations.

**Table 1.** Clinical characteristics of pancreatic cancer patients in the training and test groups are compared.

Covariates	Type	Total N (%)	TestN (%)	TrainN (%)	P-value
Age(year)	<=65	232 (62.7)	118 (63.8)	114 (61.6)	0.7
Age(year)	>65	138 (37.3)	67 (36.2)	71 (38.4)	
Gender	Female	121 (32.7)	61(32.9)	60 (32.4)	1.0
Gender	Male	249 (67.3)	124 (67.0)	125 (67.6)	
Grade	G1	55 (14.86)	29 (15.7)	26 (14.1)	0.7
Grade	G2	177 (47.84)	83 (44.9)	94 (50.8)	
Grade	G3	121 (32.7)	64 (34.6)	57 (30.8)	
Grade	G4	12 (3.2)	7 (3.8)	5 (2.7)	
Grade	unknow	5 (1.3)	2 (1.1)	3 (1.6)	
Stage	Stage I	171(46.2)	80 (43.24)	91 (49.2)	0.6
Stage	Stage II	85 (22.9)	43 (23.2)	42 (22.7)	
Stage	Stage III	85 (22.9)	47 (25.4)	38 (20.5)	
Stage	Stage IV	5 (1.4)	3 (1.6)	2 (1.1)	
Stage	unknown	24 (6.5)	12 (6.5)	12 (6.5)	
T	T1	181(48.9)	84 (45.4)	97 (52.4)	0.3
T	T2	93 (25.1)	47(25.4)	46(24.9)	
T	T3	80 (21.6)	43(23.2)	37(20)	
T	T4	13 (3.5)	9 (4.8)	4 (2.2)	
T	unknown	3 (0.8)	2(1.1)	1 (0.5)	
M	M0	266 (71.9)	126(68.1)	140 (75.7)	0.6
M	M1	4 (1.1)	3 (1.6)	1 (0.5)	
M	unknown	100 (27.0)	56 (30.3)	44 (23.8)	
N	N0	252 (68.1)	126 (68.1)	126 (68.1)	1.0
N	N1	4 (1.1)	2 (1.1)	2 (1.1)	
N	unknown	114 (30.8)	57 (30.8)	57 (30.8)	

## Discussion

In this work, a predictive model was created by combining the clinical data (time and status of survival) of liver cancer patients with the expression matrix of 168 immune checkpoint-related basement membrane genes. To create a risk model to evaluate the prognostic risk of liver cancer patients, the immune checkpoint-related basement membrane genes ADAMTS5, CTSA, FBLN5, and P3H14 were chosen. Based on the median prognostic risk grade score, they were then divided into low risk (PRG score median) and high risk (PRG score > median) groups. The Train group and the test group shared the same clinical characteristics, according to the grouping's clinical statistical to the groupng's clinical statistical analysis. According to a survival analysis, patients of the high-risk overall had a significantly poor sur-

vival rate than the patients in the latter group. There were fewer liver cancer patients in the high-risk group. As per the progression-free survival analysis survival rate of patients in the high-risk group was lower than the ones in the low-risk group. According to the risk curve, the death rate for patients with liver cancer rises as the risk score does. The three high-risk genes—ADAMTS5, CTSA, and P3H1—as well as the low-risk gene, FBLN5, can be seen on the risk heatmap. The model in this study may be an independent prognostic factor independent of other clinical features, according to both the univariate independent prognostic analysis and the multivariate independent prognostic analysis. The ROC curve values at 1, 3, and 5 years are all more than 0.5, demonstrating the remarkable accuracy of the model developed in this study in predicting patient survival. The prognostic model's area

under the ROC curve has the biggest area under it when paired with additional clinical features. The model used in this study has the biggest value for the Concordance index, indicating that it is the most accurate at predicting patients' survival times for liver cancer. The clinical grouping model showed that both patients with early-stage liver cancer and those with advanced liver cancer can use the model created in this study. According to the results of principal component analysis, the immune checkpoint-related basement membrane genes used in the model's creation were able to discriminate patients in the both risk groups quite well, although all other genes and immune checkpoint-related genes failed to do so. Among the two groups, our study further scanned 49 differential genes. The differential genes were primarily enriched in active transmembrane transporter activity, basal cell structure, and control of cyclin-dependent protein kinase activity, according to GO functional enrichment analysis. The modulation of cyclin-dependent protein kinase activity has been the subject of considerable prior research. According to Poluha<sup>10</sup>, differentiated neurocytoma cells need the cyclin-dependent kinase inhibitor p21 (WAF1) to survive. The differential genes were primarily enriched in cell-substrate adhesion and reaction to xenobiotic stimuli, according to KEGG pathway enrichment analysis. The shift in cell-substrate adhesion is a marker of cancer spreading, according to Maan et al.<sup>11</sup>. Through experimentation, Hwang<sup>12</sup> and colleagues discovered that dysregulation of cell-matrix adhesion can cause mistakes in the establishment and maintenance of tissue patterns during development, which can then result in cancer cell invasion and metastasis. Type II IFN Response, Cytolytic activity, MHC class I, and Type I IFN Response were shown to have immune-related functions having significant statistical differences between the two risk groups, and MHC class I was observed to be more active in the high-risk group. McDonald et al.<sup>13</sup> discovered that breast cancer patients with high KAM scores had higher

proportions of both pro- and anti-tumor immune cells, as well as higher levels of cytolytic activity. The loss of MHC-I APM is a frequent factor in cancer immunotherapy resistance, and Demel et al. discovered that active SUMOylation results in immune evasion in cancer by limiting MHC class I antigen presentation<sup>14</sup>. According to Zhang, M<sup>15</sup> head and neck squamous cell carcinoma has higher MHC class I expression when BET inhibition is present. The study also discovered that the four genes i.e., TP53, CTNNB1, TTN, and MUC16 had the highest mutation frequency. The mutation frequencies of the other genes, with the exception of CTNNB1, in comparison to the two risk groups was higher in the high risk one. Tumor mutational load, which is the total number of somatic or acquired mutations per million bases in a particular area of the tumor genome, and transcriptome expression both have prognostic significance in patients receiving immune checkpoint inhibitor therapy for colon cancer<sup>16,17</sup>. A possible biomarker for immunotherapy susceptibility and prognosis in patients with low-grade gliomas has also been identified as tumor mutational burden<sup>18-20</sup>. According to the findings of this study's survival analysis of tumour mutational burden, high tumour mutational burden groups' patients had a noticeably inferior survival rate as compared to the patients in the low tumour mutational burden group. An integrated survival study that took into account both of these parameters showed that patients with high tumour mutational burden and high risk scores had the lowest survival rates. Additionally, in this research a nomogram was developed using clinical characteristics and risk scores to predict survival in patients with HCC 1, 3, and 5. Patients' sensitivity with high- and low-risk liver cancer to 25 chemotherapy medications currently used to treat tumours was assessed, and it was discovered that the disparities were significant in drug sensitivity among the two risk groups for these patients. Our created immune checkpoint gene-related basement membrane gene prognosis model provides a fresh approach and concept for estimating the survival time of liver cancer patients.



Our study unavoidably includes some shortcomings and restrictions. Immune checkpoint genes and genes related to the basement membrane still have unknown molecular processes. In the future, we'll work to improve the model's accuracy by running more outside trials to validate it.

This study, a predictive model was created utilising the expression matrix of 168 genes connected to the basement membrane immune checkpoint and the HCC patients' clinical information. It is anticipated that the risk prognostic model created in this study, which is based on the relationship between immune checkpoint genes and basement membrane genes, will be used to clinically anticipate the diagnosis and treatment and immunotherapeutic reactions of liver cancer patients and provide a new strategy for survival prediction. Give patients with liver cancer additional information and strategies for their immunological treatment.

### Conclusion

It offers new insights and methodologies for the survival prediction of liver cancer patients as well as the development of immune-tailored therapies by examining the relationship between immune checkpoint gene-associated basement membrane genes and the prognosis and immunity of liver cancer patients.

### Conflict of Interest

Authors have no conflict of interest and no grant/funding from any organization

### References

- Villanueva A. Hepatocellular Carcinoma. *N Engl J Med* 2019; 380: 1450-62. [DOI:10.1056/NEJMr1713263]. Available from: [https://www.nejm.org/doi/10.1056/NEJMr1713263?url\\_ver=Z39.88-2003&rfr\\_id=ori:rid:cr ossref.org&rfr\\_dat= cr\\_pub %20%20pubmed](https://www.nejm.org/doi/10.1056/NEJMr1713263?url_ver=Z39.88-2003&rfr_id=ori:rid:cr ossref.org&rfr_dat= cr_pub %20%20pubmed). Accessed on 29<sup>th</sup> November 2022.
- Zhang Y, Zhang X, Kuang M and Yu J. Emerging insights on immunotherapy in liver cancer. *Anti oxid Redox Signal* 2022;25. [DOI: 10.1089/ars.2022.0047]. Available from: [https://www.liebertpub.com/Doi/10.1089/ars.2022.0047?url\\_ver=Z39.88-2003&rfr\\_id=ori%3Arid%3Acrossref.org&rfr\\_dat=cr\\_pub++0pubmed](https://www.liebertpub.com/Doi/10.1089/ars.2022.0047?url_ver=Z39.88-2003&rfr_id=ori%3Arid%3Acrossref.org&rfr_dat=cr_pub++0pubmed). Accessed on 29<sup>th</sup> November 2022.
- Jiang YY, Wu S, Wu YW, Gao Y, Chong D, Sun C, et al. New brefeldin A-cinnamic acid ester derivatives as potential antitumor agents: Design, synthesis and biological evaluation. *Eur J Med Chem* 2022; 240: 114598. [DOI: 10.1016/j.ejmech.2022.114598]. Available from: <https://www.science direct.com/science/article/abs/pii/S0223523422005001?via%3Dihub>. Accessed on 29<sup>th</sup> November 2022.
- Dobosz P, Stempor PA, Ramirez Moreno M and Bulgakova NA. Transcriptional and post-transcriptional regulation of checkpoint genes on the tumour side of the immunological synapse. *Here dity(Edinb)2022;129:64-74*. [DOI: 10.1038/s41437-022-00533-1]. Available from: <https://www.nature.com/articles/s41437-022-00533-1>. Accessed on 29<sup>th</sup> November 2022.
- Hu FF, Liu CJ, Liu LL, Zhang Q and Guo AY. Expression profile of immune checkpoint genes and their roles in predicting immunotherapy response. *Brief Bioinform* 2021; 22: [DOI: 10.1093/bib/bbaa176]. Available from: <https://academic.oup.com/bib/article-abstract/22/3/bbaa176/5894466?redirectedFrom=fulltext&login=false>. Accessed on 29<sup>th</sup> November 2022.
- Nystrom A, Bornert O and Kuhl T. Cell therapy for basement membrane-linked diseases. *Matrix Biol* 2017;22(3):124-39. [DOI:10.1016/j.matbio.2016.07.012]. Available from: [https://linkinghub.elsevier.com/retrieve/pii/S0945-053X\(16\)30068-3](https://linkinghub.elsevier.com/retrieve/pii/S0945-053X(16)30068-3). Accessed on 29<sup>th</sup> November 2022.
- Randles M, Lausecker F, Kong Q, Suleiman H, Reid G, Kolatsi-Joannou M, et al. Identification of an Altered Matrix Signature in Kidney Aging and Disease. *J Am Soc Nephrol* 2021;32(7):1713-2. [DOI: 10.1681/ASN.2020101442]. Available from: <https://jasn.asnjournals.org/content/32/7/1713.long>. Accessed on 29<sup>th</sup> November 2022.
- Foster MH. Basement membranes and autoimmune diseases. *Matrix Biol* 2017; 57-58: 149-168. [DOI:10.1016/j.matbio.2016.07.008]. Available from: <https://www.ncbi.nlm.nih.gov/pmc/articles/PMC5290253/pdf/nihms810300.pdf>. Accessed on 29<sup>th</sup> November 2022.
- Jayadev R, Morais MRPT, Ellingford JM, Srinivasan S, Naylor RW, Lawless C, et al. Genomics England Research Consortium, Sherwood DR, Lennon R. A basement membrane discovery pipeline uncovers network complexity, regulators, and human disease associations. *Sci Adv*. 2022 May 20;8(20):eabn2265. [DOI: 10.1126/sciadv.abn2265]. Available from: <https://www.science.org/doi/10.1126/sciadv.abn2265>. Accessed on 29<sup>th</sup> November 2022.



10. Poluha W, Poluha DK, Chang B, Crosbie NE, Schonhoff CM, Kilpatrick DL, et al. The cyclin-dependent kinase inhibitor p21 (WAF1) is required for survival of differentiating neuroblastoma cells. *MolCell Biol.* 1996 Apr;16(4):1335-41. [DOI: 10.1128/MCB.16.4.1335]. Available from: <https://www.ncbi.nlm.nih.gov/pmc/articles/PMC231117/>. Accessed on 29<sup>th</sup> November 2022.
11. Maan R, Rani G, Menon GI and Pullarkat PA. Modeling cell-substrate de-adhesion dynamics under fluid shear. *Phys Biol* 2018; 15: 046006. [DOI: 10.1088/1478-3975/aabc66]. Available from: <https://iopscience.iop.org/article/10.1088/1478-3975/aabc66>. Accessed on 29<sup>th</sup> November 2022.
12. Hwang YS, Daar IO. A frog's view of EphrinB signaling. *Genesis.* 2017 Jan;55(1-2):10.1002/dvg.23002. [DOI:10.1002/dvg.23002]. Available from: <https://onlinelibrary.wiley.com/doi/abs/10.1002/dvg.23002>. Accessed on 29<sup>th</sup> November 2022.
13. McDonald KA, Oshi M, Kawaguchi T, Qi Q, Peng X, Yamada A, et al. Development of KAM score to predict metastasis and worse survival in breast cancer. *Am J Cancer Res.* 2021 Nov 15;11 (11):5388-5401. Available from: <https://www.ncbi.nlm.nih.gov/pmc/articles/PMC8640803/>. Accessed on 29<sup>th</sup> November 2022.
14. Demel UM, Boger M, Yousefian S, Grunert C, Zhang L, Hotz PW, et al. Activated SUMOylation restricts MHC class I antigen presentation to confer immune evasion in cancer. *J Clin Invest* 2022; 132:1-16. [DOI:10.1172/JCI152383]. Available from: <https://www.jci.org/articles/view/152383/pdf>. Accessed on 29<sup>th</sup> November 2022.
15. Zhang M, Wang G, Ma Z, Xiong G, Wang W, Huang Z, et al. BET inhibition triggers antitumor immunity by enhancing MHC class I expression in head and neck squamous cell carcinoma. *Mol Ther* 2022;30(11):3394-3413. [DOI: 10.1016/j.yjmt.2022.07.022]. Available from: [https://www.cell.com/molecular-therapy-family/molecular-therapy/fulltext/S1525-0016\(22\)00443-9](https://www.cell.com/molecular-therapy-family/molecular-therapy/fulltext/S1525-0016(22)00443-9). Accessed on 29<sup>th</sup> November 2022.
16. Liang L, Jiang W, Zheng Y, Liu T, Shen X, Chen Y. Integrating tumor mutational burden and transcriptome expression into prediction of immune checkpoint inhibitor response and prognosis of patients with colon cancer. *J Physiol Pharmaco* 2022;73(2):203-18. [DOI:10.26402/jpp.2022.2.04]. Available from: [https://www.jpp.krakow.pl/journal/archive/04\\_22/pdf/10.26402/jpp.2022.2.04.pdf](https://www.jpp.krakow.pl/journal/archive/04_22/pdf/10.26402/jpp.2022.2.04.pdf). Accessed on 29<sup>th</sup> November 2022.
17. Quin L, Zhou Q, Zhao S, Wu P, Shi P, Zeng J, et al., KRAS mutation predict response and outcome in advanced non-small cell lung carcinoma without driver alterations receiving PD-1 blockade immunotherapy combined with platinum-based chemotherapy: a retrospective cohort study from China. *Transl Lung Cancer Res*, 2022;11(10):2136-47. [DOI: 10.21037/tlcr-22-655]. Available from: <https://tlcr.amegroups.com/article/view/69407/html>. Accessed on 29<sup>th</sup> November 2022.
18. Lam LHT, Chu NT, Tran TO, Do DT and Le NQK. A Radiomics-Based Machine Learning Model for Prediction of Tumor Mutational Burden in Lower-Grade Gliomas. *Cancers (Basel)* 2022;14:2-14. [DOI: 10.3390/cancers14143492]. Available from: <https://www.mdpi.com/2072-6694/14/14/3492>. Accessed on 29<sup>th</sup> November 2022.
19. Yu D, Yuan C, Zhang H and Chu W. The association of efficacy with PD-1/PD-L1 inhibition and tumor mutational burden in advanced non-small cell lung cancer: A PRISMA-guided literature review and meta-analysis. *Medicine (Baltimore)* 2022; 101:e29676. [DOI:10.1097/MD.00000000000029676]. Available from: [https://journals.lww.com/md-journal/Fulltext/2022/07220/The\\_association\\_of\\_efficacy\\_with\\_PD\\_1\\_PD\\_L1.36.aspx](https://journals.lww.com/md-journal/Fulltext/2022/07220/The_association_of_efficacy_with_PD_1_PD_L1.36.aspx). Accessed on 29<sup>th</sup> November 2022.
20. Abate RE, Cheetham MH, Fairley JA, Pasquale R, Sacco A, Nicola W, et al. External quality assessment (EQA) for tumor mutational burden: results of an international IQN path feasibility pilot scheme. *Virchows Arch*, 2022. [DOI: 10.1007/s00428-022-03444-y]. Available from: <https://link.springer.com/article/10.1007/s00428-022-03444-y>. Accessed on 29<sup>th</sup> November 2022